CrossMark

ORIGINAL ARTICLE

Identification of hydrogeochemical processes and pollution sources of groundwater resources in the Marand plain, northwest of Iran

Rahim Barzegar[1] · Asghar Asghari Moghaddam[1] · Evangelos Tziritis[2] ·
Mir Sajjad Fakhri[1] · Shahla Soltani[1]

Abstract The main aims of the present study are to identify the major factors affecting hydrogeochemistry of groundwater resources in the Marand plain, NW Iran and to evaluate the potential sources of major and trace elements using multivariate statistical analysis such as hierarchical clustering analysis (HCA) and factor analysis (FA). To achieve these goals, groundwater samples were collected in three sampling periods in September 2013, May 2014 and September 2014 and analyzed with regard to ions (e.g., Ca^{2+}, Mg^{2+}, Na^+ and K^+, HCO_3^-, SO_4^{2-}, Cl^-, F^- and NO_3^-) and trace metals (e.g., Cr, Pb, Cd, Mn, Fe, Al and As). The piper diagrams show that the majority of samples belong to Na–Cl water type and are followed by Ca–HCO_3 and mixed Ca–Na–HCO_3. Cross-plots show that weathering and dissolution of different rocks and minerals, ion exchange, reverse ion exchange and anthropogenic activities, especially agricultural activities, influence the hydrogeochemistry of the study area. The results of the FA demonstrate that 6 factors with 81.7% of total variance are effective in the overall hydrogeochemistry, which are attributed to geogenic and anthropogenic impacts. The HCA categorizes the samples into two clusters. Samples of cluster C1, which appear to have higher values of some trace metals like Pb and As, are spatially located at the eastern and central parts of the plain, while samples of cluster C2, which express the salinization of the groundwater, are situated mainly westward with few local exceptions.

Keywords Hydrogeochemistry · Trace metals · Multivariate statistical analysis · Marand plain · NW Iran

Introduction

Groundwater is a significant source of water supply for domestic, industrial and agricultural sectors in both urban and rural regions in many countries throughout the world. Its chemical composition, especially in the arid and semi-arid regions, is chiefly affected and controlled by natural process (e.g., local hydrology–hydrogeology, rock–water interactions, evaporation, dissolution and deposition of minerals, groundwater flow and interaction with other types of aquifers) and anthropogenic activities (e.g., industry, agriculture, mining and urbanization) (Sajil Kumar 2014). Naturally, groundwater is usually free from contamination, but anthropogenic activities can impact significantly on the quality; hence, interventions are needed prior to its usage (Yidana et al. 2012). The quality of groundwater is characterized by different physicochemical features and constitutes the final result of all the processes and reactions that act on the water from the moment it condenses in the atmosphere to the time it is discharged by a well (Arumugam and Elangovan 2009; Pichaiah et al. 2015; Pandey 2016).

Understanding of the hydrogeochemical processes and contamination sources and regular monitoring of water quality are essential for sustainable development and effective management of groundwater resources (Tiwari and Singh 2014). Various methods such as different graphical techniques (e.g., Piper, Durov, Stiff diagrams)

✉ Rahim Barzegar
  rm.barzegar@yahoo.com

[1] Department of Earth Sciences, Faculty of Natural Sciences, University of Tabriz, Tabriz, Iran

[2] Hellenic Agricultural Organization, Soil and Water Resources Institute, 57400 Sindos, Greece

and bivariate or scatter plots that have been developed for the visual understanding of hydrogeochemical data in order to show water classification, sources of water solutes, reveal the discernible patterns, trends, dissimilarities of water composition and quality (Dalton and Upchurch 1978; Sadashivaiah et al. 2008).

In recent years, multivariate statistical techniques such as clustering analysis (CA) and factor analysis (FA) have been used to identify geochemical controls on the composition of groundwater (Tziritis 2014; Varol and Davraz 2015; Hassen et al. 2016) and determine anomalies resulting from different impacts, such as anthropogenic and geogenic (Hernandez et al. 1991; Birke and Rauch 1993; Helena et al. 2000; Pereira et al. 2003) on a variety of scales. Clustering analysis (CA) is a group of multivariate techniques whose primary purpose is to assemble objects using predetermined selection criterion to classify objects in clusters that exhibit high internal (within cluster) homogeneity and high external (between clusters) heterogeneity (McKenna 2003). The levels of the similarity at each observation are used to construct a dendrogram (Lokhande et al. 2008). The dendrogram provides a visual summary of clustering process, presenting a picture of groups and their proximity, with a dramatic reduction in dimensionality of the original data. Factor analysis methods allow a reduction in the number of variables that describe system behavior and the identification of new, homogeneous subgroups that are easier to identify (Lawrence and Upchurch 1982; Al-Qudah et al. 2011).

In last decades, water crisis has occurred in Iran due to several reasons including rapid population growth which is disproportional to the environmental capacity, development of agriculture, industry and urbanization, decrease in the number of appropriate structures to store, distribute and convey water and worldwide occurrence of drought (i.e., Iran) since 1995 (Manouchehri 2000; Motiee et al. 2001). Water shortages have become an increasingly serious problem, especially in the arid and semiarid regions of western Iran (Jalali 2006; Pazand et al. 2012). Therefore, understanding the groundwater quality and its hydrogeochemical properties is of great importance for the sustainable management of groundwater resources.

Marand plain is one of the fertile plains of East Azarbaijan Province, NW Iran. In the last decades, rapid population growth and agricultural development and recent droughts have tremendously increased pressure on groundwater resources. Although the groundwater is the main resource for irrigation and drinking, very few studies have dealt with the hydrogeochemistry, especially trace metals. Pazand et al. (2012) evaluated the geochemistry and quality of the groundwater in the Marand basin. Khaleghi and Shahverdizadeh (2014) assessed the water quality of the Marand plain for the purpose of drinking and irrigation. Fakhri et al. (2015) investigated the nitrate concentration in the groundwater of the Marand plain and applied AVI and GODS methods for assessment of the groundwater intrinsic vulnerability.

With the above backgrounds, the main objectives of the present study are to identify the major processes affecting hydrogeochemistry of groundwater resources and to evaluate the potential sources of major and trace elements using multivariate statistical techniques, such as hierarchical clustering analysis (HCA) and factor analysis (FA).

Materials and methods

Study area

Marand plain, with an area of approximately 826 Km^2, is located in northwest Iran's East Azarbaijan province. The plain is a sub-basin of the Caspian Sea basin and bordered to the north by Ghezel-Dagh and Ghaleh-Dagh Mountain ranges, to the west by Zonouz-Chay and Zilbir-Chay rivers, to the south by the Mishow and Pir-Dagh Mountain ranges (Fig. 1). The plain is restricted between the highlands with a moderate slope (2–5%) from northern, southern and eastern highlands toward the center and western of the plain.

Generally, the majority of precipitation in the area occurs during the autumn, winter and spring; from the third month of autumn (December) till the end of winter (March), it falls as snow rather than rain. The mean annual precipitation is 242.7 mm. The mean annual temperature is 11.4 °C, ranging from 36 °C in the summer (July) to −12.4 °C in the winter (January). The monthly evapotranspiration (ET) rate varies between 5 mm/month in winter and 370 mm/month in summer. Based on the Emberger climate classification, the climate of the area is defined as cold and dry (Fakhri et al. 2015).

Marand plain is of great importance in the region due to agricultural activities and population density. The population has increased from 36,108 in 1976 to 239,209 in 2011. Groundwater is the primary source of fresh water for drinking, agricultural, domestic and industrial uses in the area. Hence, water quality is a critical factor affecting socioeconomic welfare, apart from the direct environmental pressures.

Geological and hydrogeological setting

The Marand plain lies between the Alborz and Azarbaijan zones of Iran (Nabavi 1976) and is a part of the Central Iran structural units (Berberian 1976). The geological map of the Marand basin is shown in Fig. 2 (adopted from Eftekhar Nezhad et al. 1991). The exposed lithological units of

Fig. 1 Location map of the study area
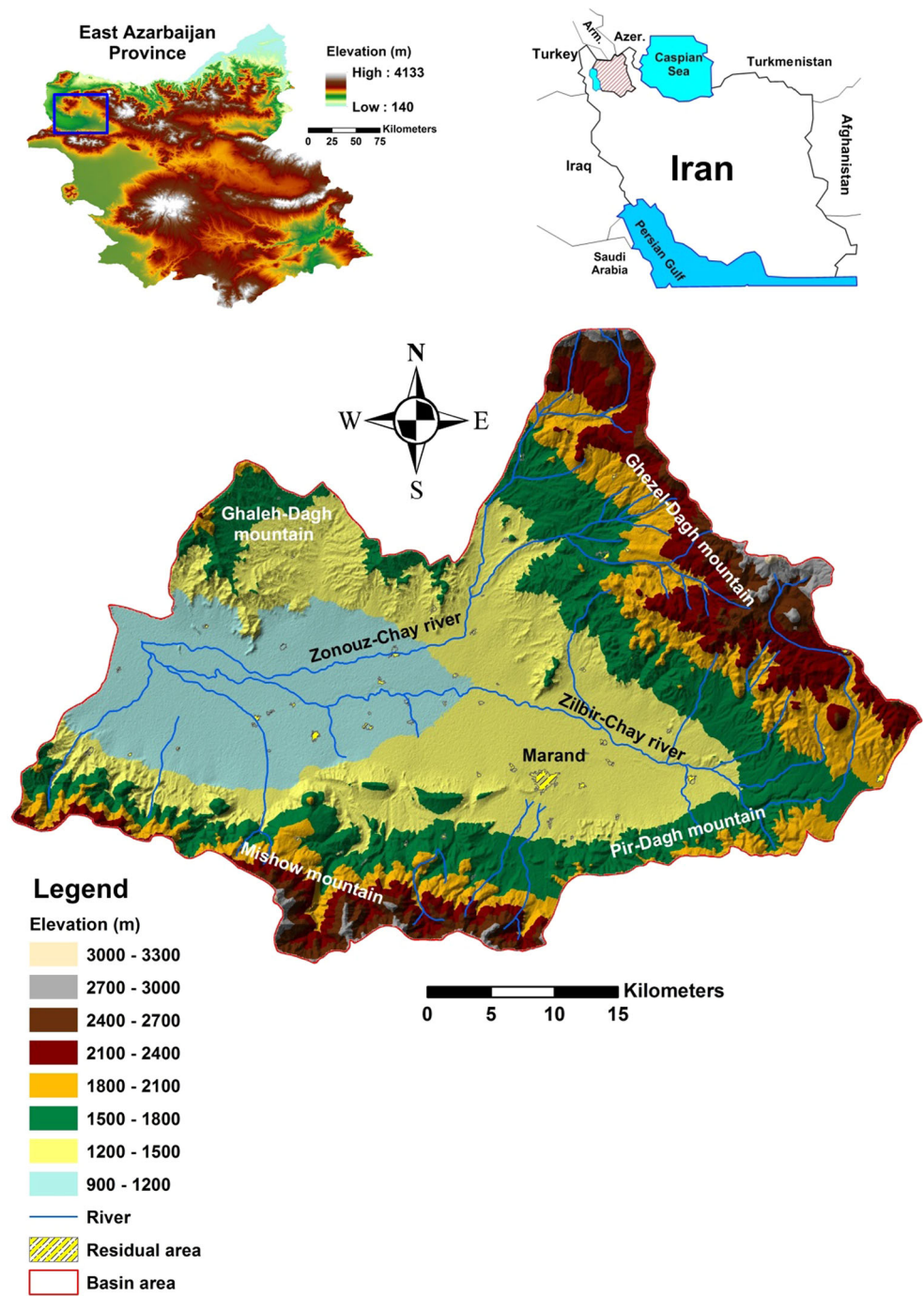
the area range in age from Pre-Cambrian to Quaternary. The oldest geologic units in the study area are Pre-Cambrian shales and consist of mica shales, schists, dolostones, sandstones, tuffs, rhyolites, andesites, metamorphic rocks and intermediate layers of crystalline limestones and cherts, which are situated in the shout of the plain.

Volcanic formations like chlorite-schists, lava, rhyolites, tuffs and andesite, as well as Pliocene conglomerates and sandstones are outcropped and situated unconformity on different units of the Miocene, in the northern slopes of the

Mishow Mountain. Also, volcanic formations of Tertiary age including andesites and basalts with sandstone and limestones are exposed in the northeast of the plain (Eftekhar Nezhad et al. 1991).

The central parts of the study area are plain regions, which are covered by Quaternary alluvial deposits and surrounded by conglomerates (Eftekhar Nezhad et al. 1991; Pazand et al. 2012).

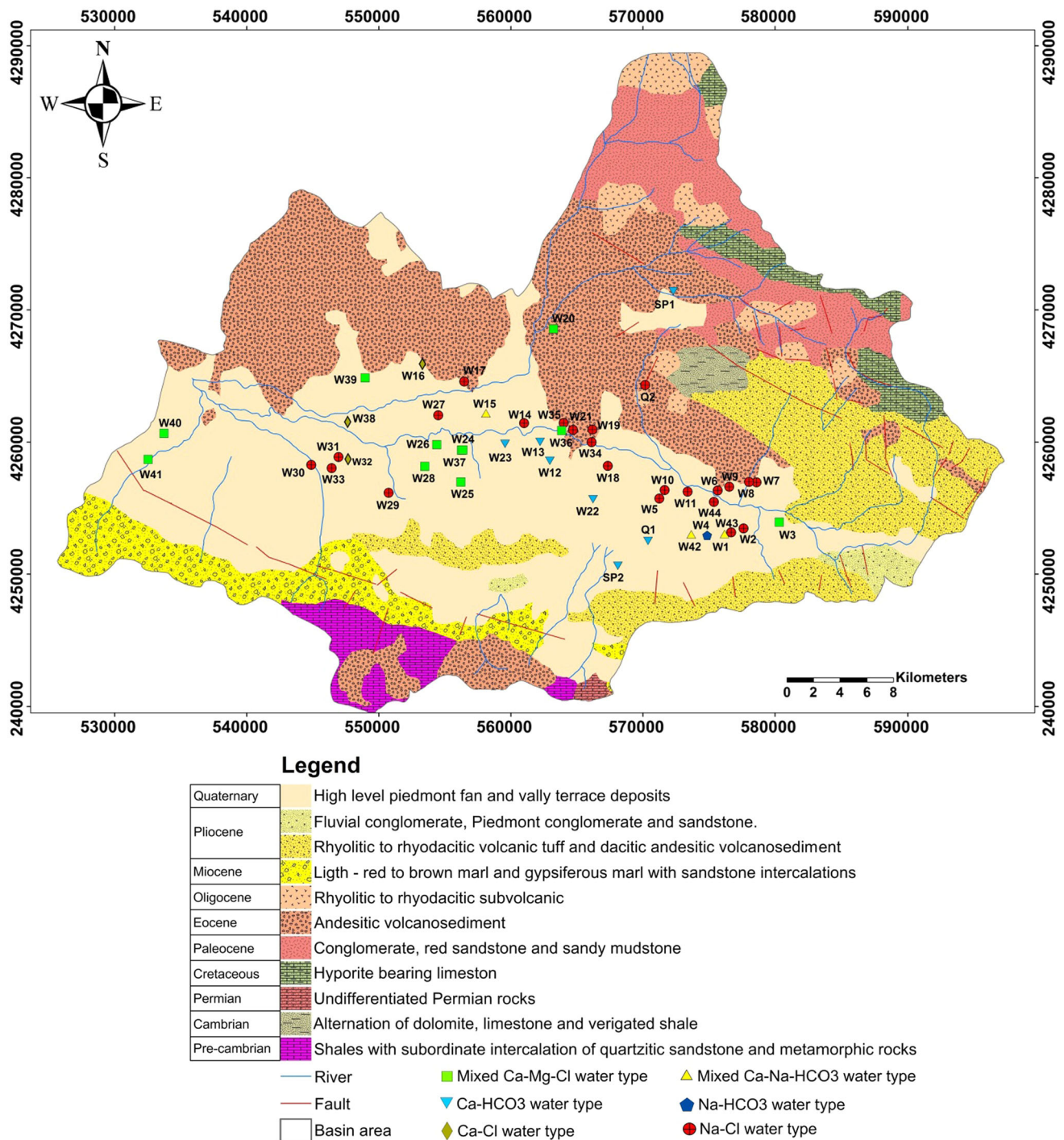Zilbir-Chay and Zonouz-Chay are the most important rivers in the study area. These rivers originate from

Fig. 2 Map of the study area showing geological units and sampling points with water types

southern slopes of Sultan–Jahangir Mountain and western slopes of Kiamaki-Dagh Mountain, respectively. Zilbir-Chay River flows in an east–west direction in the plain. Zonouz-Chay River enters the plain from the north and joins the Zilbir-Chay in the west and finally, exits from the plain and flows to the Aras River (Fakhri et al. 2015).

Based on the results of geophysical investigations and geological logs, there are three types of aquifer systems developed in the plain area, including an unconfined, a semi-confined and a confined aquifer (Fig. 1). The unconfined aquifer is developed at the eastern part of the plain area where alluvial deposits are course without many gradation changes; it is developed within old and recent

terraces, alluvial fans and fluvial sediments composed of gravel, sand, silt and clay. The thickness of the unconfined aquifer varies between 220 and 270 m in the east and southeast of the plain and reaches to <40 m in the center of the plain. At the southern part of the plain is developed a semi-hard conglomerate formation with Plio–Pleistocene debris of low permeable and semi-permeable regions because of clay and marl layers. The confined aquifer, mostly in the form of alluvial deposits, is covered by clay and marl layers with thicknesses varying from 10 to 30 m. The maximum thickness of the confined aquifer reaches 170 meters in some parts of the plain. The confined aquifer is located in the central and western plain area, as well as in some parts of the Zilbir-Chay and Zonouz-Chay Rivers terraces. The semi-confined aquifer is placed in western part of the plain; its thickness varies between 10 and 150 m (Fakhri et al. 2015). Figure 3 shows six geological cross sections of the different layers of alluvial deposits, which were deduced from the geophysical investigations; the location of the geoelectrical sondes is illustrated in Fig. 4. Groundwater resources of the plain have been formed in quaternary alluvial deposits. Figure 4 shows the schematic positions of the aquifers in the Marand plain.

Generally, the regional groundwater flow direction follows the topography of the area, mainly from the highlands to the center and from east to the west of the plain (Fig. 5). In general, the aquifer systems are fed by precipitation, recharge from the rivers, groundwater return flows from irrigation and groundwater lateral cross-flows from the surrounding mountains (Fakhri et al. 2015). Discharge occurs by base flow to the Zilbir-Chay River and also artificially through water galleries known locally as "qanat." Abstractions are via dug wells which supply water for agricultural and drinking purposes. In the last 20 years, the groundwater levels have declined because of extensive abstraction and low recharge. Pumping and recovery tests showed that transmissivity is in the range 25–945 m²/day and the storage coefficient 0.0625 (Fakhri et al. 2015).

The bedrock of the plain consists of conglomerate in the east and southeast, silt, sandstone, granites, andesite, basalt and schist in the north and limestone and gypsum in the west.

Water sampling and analysis

Groundwater samples were collected from shallow and deep wells, springs and qanats in three sampling periods in September 2013, May 2014 and September 2014 ($n = 48$ and 27 for major ions and trace metals analysis, respectively). Figure 2 illustrates the location of the sampling points. To conduct the sampling, two separate polyethylene bottles were used for samples of major ions and trace elements. Each polyethylene bottle was rinsed three times with the subsequent water sample prior to sampling, to prevent potential elemental contamination from the bottle during storage. Water samples for trace metals analysis were acidified by adding 2 mL of HNO_3 50%.

The pH and electrical conductivity (EC) of the groundwater samples were measured in the field. The collected groundwater samples were analyzed in the laboratory for cations (Ca^{2+}, Mg^{2+}, Na^+ and K^+) and anions (HCO_3^-, SO_4^{2-}, Cl^-, F^- and NO_3^-) using the standard methods as suggested by the American Public Health Association (APHA 2005). Na^+ and K^+ were determined by flame photometer. Ca^{2+}, HCO_3^- and Cl^- were analyzed by volumetric methods and SO_4^{2-}, F^- and NO_3^- by spectrophotometry at "Hydrogeology Laboratory of University of Tabriz". Trace metals concentrations such as Cr, Pb, Cd, Mn, Fe, Al and As were analyzed by atomic absorption method at "Water Quality Control Laboratory of the East Azarbaijan Province". Statistical parameters of analyzed samples for the three sampling periods are given in Table 1.

The accuracy of the analysis was calculated from the ion balance equation (Eq. 1)

$$B = \frac{(C - A)}{(C + A)} \times 100 \tag{1}$$

where C and A are the concentrations of total cations and total anions, respectively, in meq/L, and B is the percentage of ionic balance error (Domenico and Schwartz 1998). The ion balance error did not exceed 5% in any of the sample analyses.

Multivariate statistical analysis

Multivariate statistical analysis can help to simplify and organize large data set to support meaningful insight (Yidana et al. 2008; Nesrine et al. 2015). In this study, hierarchical cluster analysis (HCA) was performed using Ward's method (Ward 1963). The Ward method uses an intra-cluster variation to form clusters, and the clusters are formed by maximizing the homogeneity within each cluster (Hardle and Simar 2007). The squared Euclidean distance criteria were used as measure of distance, which is one of the most commonly adopted measures. The squared Euclidean distance usually gives the similarity between two samples, and a distance can be represented by the difference between analytical values from the samples (Otto 1998; Bhuiyan et al. 2011).

Factor analysis (FA) uses linear combinations of the variables to form the factors with a mean of zero and standard deviation of one. In the present study, the principal component analysis (PCA) was used to extract eigenvalues and eigenvectors from the covariance matrix of original variables to produce new orthogonal variables
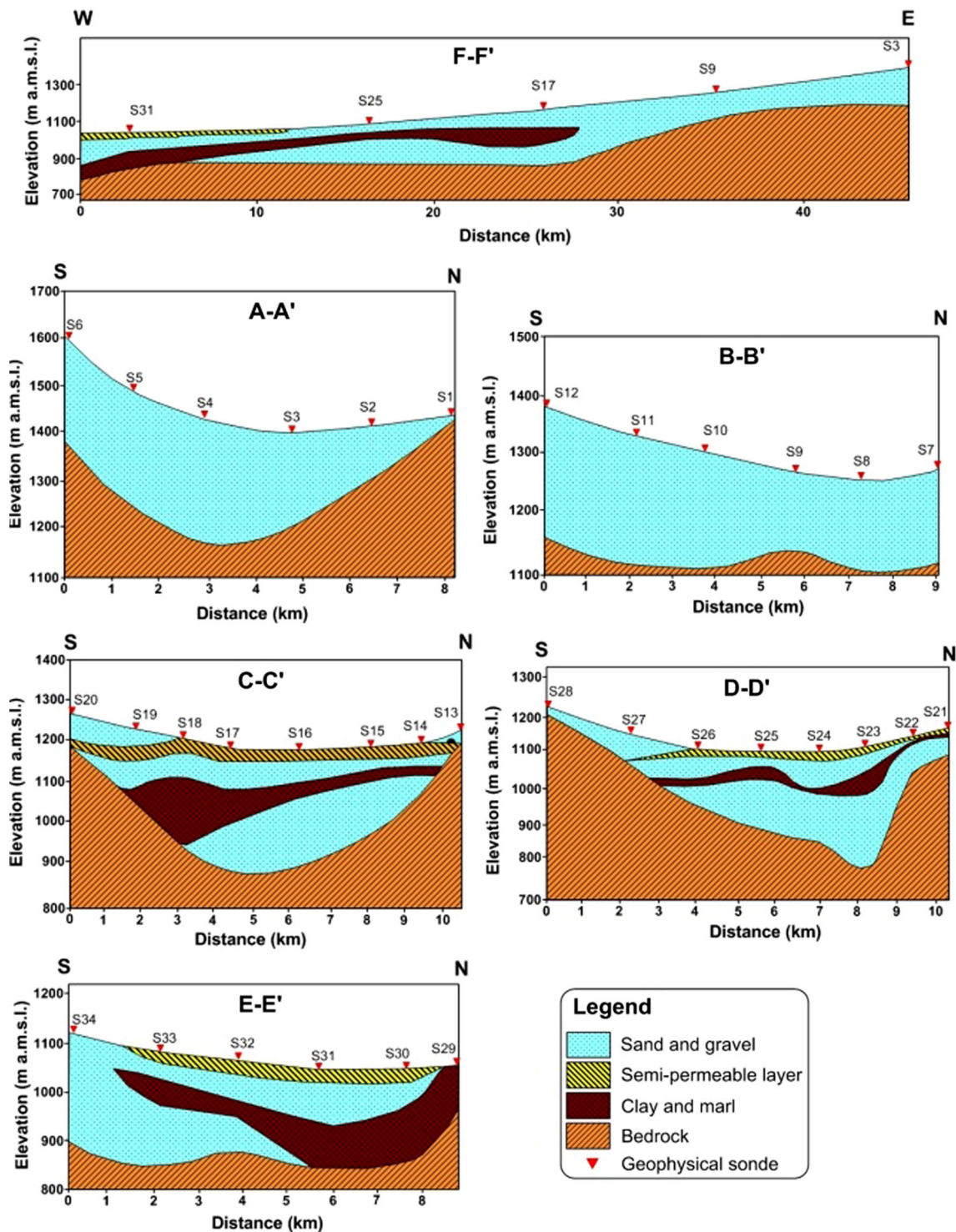
Fig. 3 Geological cross sections from the Marand plain

known as varifactors (VFs) through varimax rotation, which are linear combinations of the original variables (Devic et al. 2014). The first step in FA is to standardize the parameters for all parameters. This is due to avoid different units of parameters (Fitzpatrick et al. 2007). The most common rotation is the normalized varimax rotation, which attempts to find the rotation that will maximize variability on the rotated axes while minimizing it everywhere else (Al-Qudah et al. 2011). Finally, a scree plot is used to determine the number of PCs to be retained (Helena et al. 2000). The software package SPSS16.0 was used for statistical analysis.
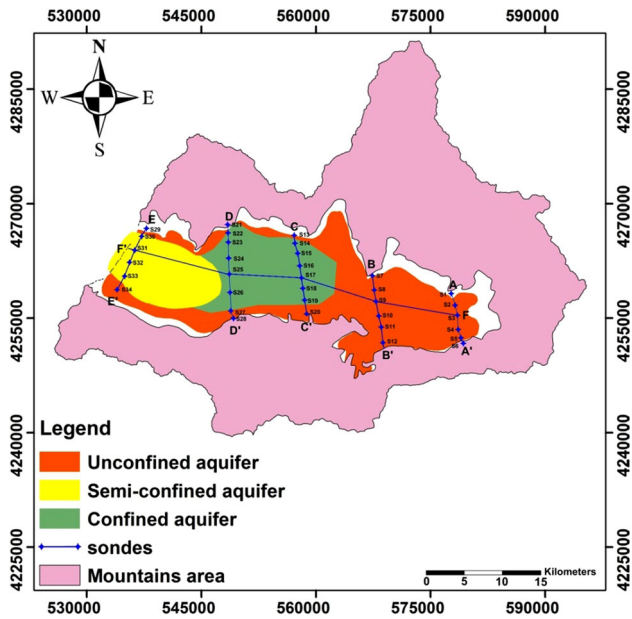
Fig. 4 Schematic positions of the aquifers and geological cross sections

Results and discussion

Hydrogeochemistry

The values of electrical conductivity (EC), which is an indirect measure of ionic strength and mineralization for natural waters, range between 377 and 5120 µS/cm for all three sampling periods; the elevated EC values >2500 µS/cm are indicative for the existence of increased groundwater salinization, a fact which should be chiefly attributed to irrigation water return flows.

Groundwater has generally circum-neutral pH (with median values of 7.4 and 7.6 for the three sampling periods); however, relatively acidic (W16) or alkaline samples (W1) exist as outliers, and their values (5.8 and 8.3, respectively) are likely to be attributed to the impact of the geological formations (felsic and mafic–ultramafic volcanic formations,

respectively). Based on the median values for all sampling periods, the order of abundance of major cations is Na^+ (150 mg/L) > Ca^{2+} (62 mg/L) > Mg^{2+} (43 mg/L) > K^+ (5 mg/L) and of major anions is HCO_3^- (286 mg/L) > Cl^- (177 mg/L) > SO_4^{2-} (89 mg/L). In respect of the trace metals, their median values (Al and Cr values accounted only for 2 periods) follow the decreasing concentration order: Al (53 µg/L) > Fe (51 µg/L) > As (12 µg/L) > Pb (11 µg/L) > Cr (6 µg/L) > Mn (5 µg/L) > Cd (2 µg/L). However, individual outliers especially for the most toxic trace elements like Pb (up to 32 µg/L), As (up to 44 µg/L) and Cd (up to 11 µg/L), denote that locally are developed significant environmental pressures related to the aforementioned parameters.

The Piper diagrams (Fig. 6) show that all water types including $Ca–HCO_3$, Na–Cl, mixed $Ca–Na–HCO_3$, mixed Ca–Mg–Cl, Ca–Cl and $Na–HCO_3$ can be found in groundwater of the Marand plain; however, the majority of samples belong to Na–Cl water type and are followed by $Ca–HCO_3$ and mixed $Ca–Na–HCO_3$. The plots show that most of the water samples fall in the field of alkalies (Na^+, K^+) dominating over the alkaline earth metals (Ca^{2+}, Mg^{2+}) and strong acid (Cl^-, SO_4^{2-}) exceed the weak acid (HCO_3^-). Most of the samples fall in field 2 which show the highest Na–Cl content. Spatially (Fig. 2) the most saline groundwaters expressed by the Na–Cl water type are located mainly in the northern and eastern parts of the plain; however, few samples are developed centrally. Mixed water types are located in inner plain areas, denoting a succession with the saline waters due to ion exchange and reverse ion exchange processes. Recharge areas, expressed by $Ca–HCO_3$ type, seem to follow a SE–NW direction across the eastern and central plain areas, implying a potential groundwater flow path.

Reactions between groundwater and aquifer matrix have a significant impact on water chemistry and can be used for identifying the origin of groundwater solutes (Subramani et al. 2010). Different processes including rock weathering, evaporation, and ion exchange can affect the chemistry of the groundwater system. To identify these processes,

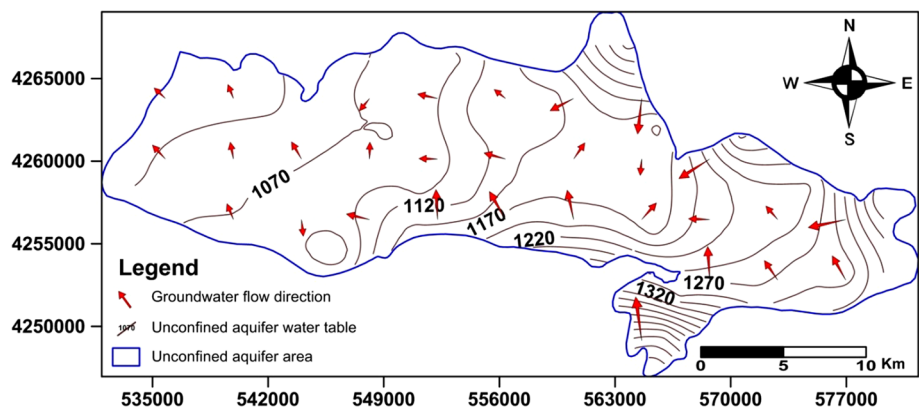**Fig. 5** Groundwater flow direction in the Marand plain

Table 1 Statistical parameters of analyzed groundwater samples for September 2013, May 2014 and September 2014 periods

	Unit	September 2013				May 2014				September 2014			
		Min.	Max.	Median	SD	Min.	Max.	Median	SD	Min.	Max.	Median	SD
pH	–	5.9	8.0	7.4	0.4	5.8	8.3	7.6	0.5	5.9	7.9	7.4	0.4
EC	µS/cm	387.0	4270.0	1121.5	1081.1	377.0	4550.0	1187.0	1168.8	430.0	5120.0	1223.5	1231.3
TDS	mg/L	248.0	2733.0	718.0	691.9	241.0	2912.0	760.0	748.1	275.0	3277.0	783.0	788.0
Ca^{2+}	mg/L	20.8	288.6	75.3	76.6	14.4	312.6	54.9	58.6	17.6	372.7	56.9	93.7
Mg^{2+}	mg/L	3.8	136.1	43.2	33.5	3.8	141.5	44.2	38.7	4.8	261.3	40.2	55.5
Na^+	mg/L	31.9	659.3	170.8	166.8	19.0	655.2	133.5	160.4	18.1	643.7	145.5	151.3
K^+	mg/L	0.4	19.9	2.7	4.1	1.9	25.4	6.2	5.3	2.3	29.7	6.6	5.5
HCO_3^-	mg/L	122.0	707.8	338.9	125.6	100.1	510.1	239.1	105.4	173.3	1114.0	280.6	190.2
SO_4^{2-}	mg/L	5.7	846.8	20.1	218.1	11.0	540.8	119.6	126.5	7.6	779.1	127.0	188.0
Cl^-	mg/L	19.5	1134.0	230.4	296.1	14.8	1205.0	160.9	286.3	13.8	959.7	140.0	260.3
NO_3^-	mg/L	4.3	95.4	13.3	20.3	1.7	155.5	10.6	23.2	1.2	85.5	13.3	12.5
SiO_2	mg/L	0.0	35.1	10.6	7.9	0.5	43.8	1.8	11.1	2.1	36.8	16.6	8.2
F^-	mg/L	0.2	4.4	0.6	0.9	0.1	0.6	0.2	0.1	0.0	0.6	0.2	0.1
Cr	µg/L	0.0	46.0	0.0	9.0	3.9	17.7	9.1	3.1	–	–	–	–
Pb	µg/L	1.0	22.0	12.0	4.6	4.0	31.5	11.0	6.5	1.0	31.0	11.0	6.9
Cd	µg/L	1.0	6.0	2.0	1.4	0.1	10.9	1.8	2.3	0.0	6.4	1.6	1.5
Mn	µg/L	0.0	525.0	6.0	101.8	0.0	790.0	0.0	181.7	0.8	1025.0	3.2	245.4
Al	µg/L	40.0	1723.0	78.0	372.7	5.0	246.0	38.0	58.3	–	–	–	–
Fe	µg/L	6.0	900.0	72.0	186.3	0.0	269.0	43.3	74.7	10.3	452.6	37.5	113.2
As	µg/L	1.0	31.0	4.0	8.7	0.0	22.0	10.0	7.5	1.0	44.0	22.0	11.8

different scatter plots can be used; previous studies (e.g., Datta and Tyagi 1996; Kumar et al. 2006; Venugopal et al. 2009) showed that if the dissolution of calcite, dolomite, anhydrite and gypsum are the dominant processes in the water system, the $Ca^{2+} + Mg^{2+}$ versus $HCO_3^- + SO_4^{2-}$ scatter plot will be close to the 1:1 equiline. As well as, the dominance of $HCO_3^- + SO_4^{2-}$ over $Ca^{2+} + Mg^{2+}$ can be indication of silicate weathering, whereas the abundance of $Ca^{2+} + Mg^{2+}$ can be an indicator of reverse ion exchange (Elango and Kannan 2007; Barzegar et al. 2016). As shown in Fig. 7a, some of the groundwater samples fall on the 1:1 line, whereas most of the samples fall on the both sides of the line, which indicates the significant impact of silicate weathering and reverse ion exchange on groundwater chemistry. In addition, the impact of silicate weathering can be found by the plot of $Na^+ + K^+$ versus total cations (TC). As shown in Fig. 7b, most of the data points are plotted above the $Na^+ + K^+ = 0.5$ TC. This indicates the involvement of silicate weathering which contributes Na^+ and K^+ to the groundwater (Stallard and Edmond 1983; Rajmohan and Elango 2004; Senthilkumar and Elango 2013); some samples deviated from $Na^+ + K^+ = 0.5$ TC line and show lower $Na^+ + K^+$ concentration, due to the Ca^{2+}/Na^+ exchange reactions (Subramani et al. 2010).

The plot of Ca^{2+} versus SO_4^{2-} was used to show the impact of gypsum dissolution on groundwater chemistry

(Fig. 7c). The plot shows that only few samples fall on the 1:1 line which indicates the dissolution of gypsum. Falling of the samples above the 1:1 line can be indication of cation exchange, whereas samples below the 1:1 line can be indication of the excess of SO_4^{2-} and probably an oxidizing hydrogeological environment (Tarki et al. 2011).

Fisher and Mulican (1997) suggested that the relationship between $Na^+ - Cl^-$ and $(Ca^{2+} + Mg^{2+} - HCO_3^- - SO_4^{2-})$ should be linear with a slope of -1.0, if reverse ion exchange is a significant geochemical process for controlling the chemistry of groundwater. Figure 7d shows that the plots define a straight line with a slope of $-1.15, -1.01$ and -1.29 for September 2013, May 2013 and September 2014, respectively. This indicates that the main contribution of reverse ion exchange process occurs in samples of May 2014. The plot of $Ca^{2+} + Mg^{2+}$ versus Na^+ (Fig. 7e) was also used for the assessment of ion exchange and revealed the presence of water samples on both sides of the 1:1 line, a fact which is an indication that ion exchange and reverse ion exchange occur jointly.

The plot of Na^+ versus Cl^- (Fig. 7f) was used to evaluate of the effect of halite dissolution on the groundwater chemistry. The plot shows that the majority of samples fall on the 1:1 equiline. This well-defined relationship and the relatively high concentrations in
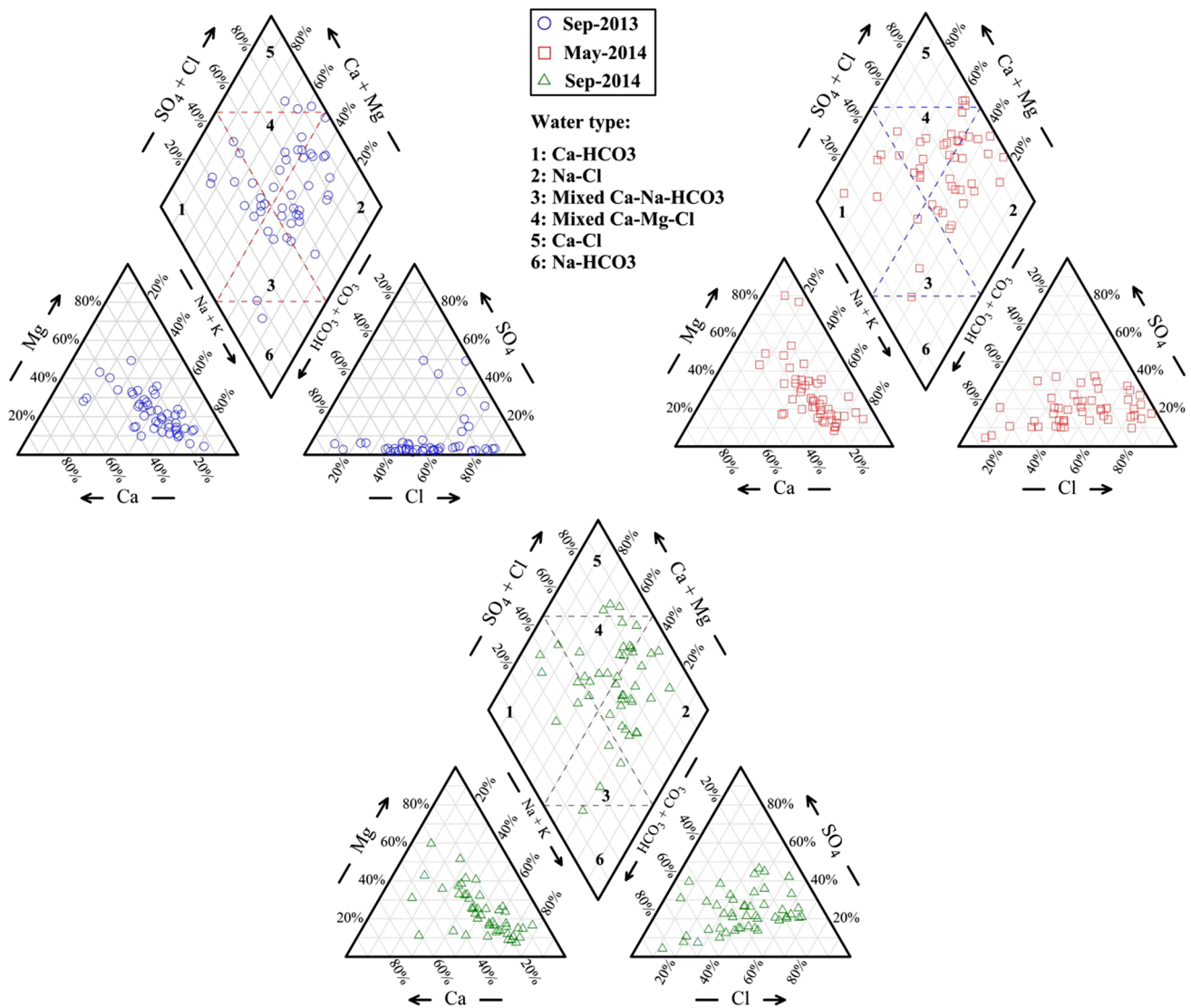
Fig. 6 Piper diagrams for groundwater samples of the three sampling periods

Na$^+$ and Cl$^-$ demonstrate the role of halite dissolution as a major process contributing to the water salinization (Appelo and Postma 1993).

Human activity is one of the most important factors affecting groundwater chemistry. The plot of TDS versus (NO$_3^-$ + Cl$^-$)/HCO$_3^-$ was used to evaluate the impact of anthropogenic activities on groundwater system. Han and Liu (2004) and Jalali (2009) suggested that the high correlation between TDS and (NO$_3^-$ + Cl$^-$)/HCO$_3^-$ reveals the influence of anthropogenic activities especially agricultural activities on water chemistry. As shown in Fig. 7f, there is a moderate to strong positive correlation between TDS values and (NO$_3^-$ + Cl$^-$)/HCO$_3^-$ for all the samples which suggests the influence of anthropogenic activities on the water. The highest correlation ($R^2 = 0.647$) is shown for the samples of May 2014. This is due to the use of the agricultural fertilizers.

To understand the groundwater interaction with precipitation (rainfall), rock weathering and evaporation, plots of log TDS against Na$^+$/(Na$^+$ + Ca^{2+}) and Cl$^-$/(Cl$^-$ + HCO$_3^-$) (Gibbs 1970) were used. As can be seen in Fig. 8, the ratios of cations Na$^+$/(Na$^+$ + Ca^{2+}) as well as the ration of anions Cl$^-$/(Cl$^-$ + HCO$_3^-$) are plotted from the rock domain toward the evaporation domain, which indicates that water–rock interaction and evaporation mechanism are affecting the groundwater compositions. In addition, a dense clustering of sample points can be seen in the evaporation domain which indicates the impact of anthropogenic activities (Li et al. 2013).

Factor analysis

The multivariate statistical method of R-mode factor analysis (FA) has been applied to groundwater data in

Fig. 7 Ions scatter diagrams for groundwater samples of the three periods
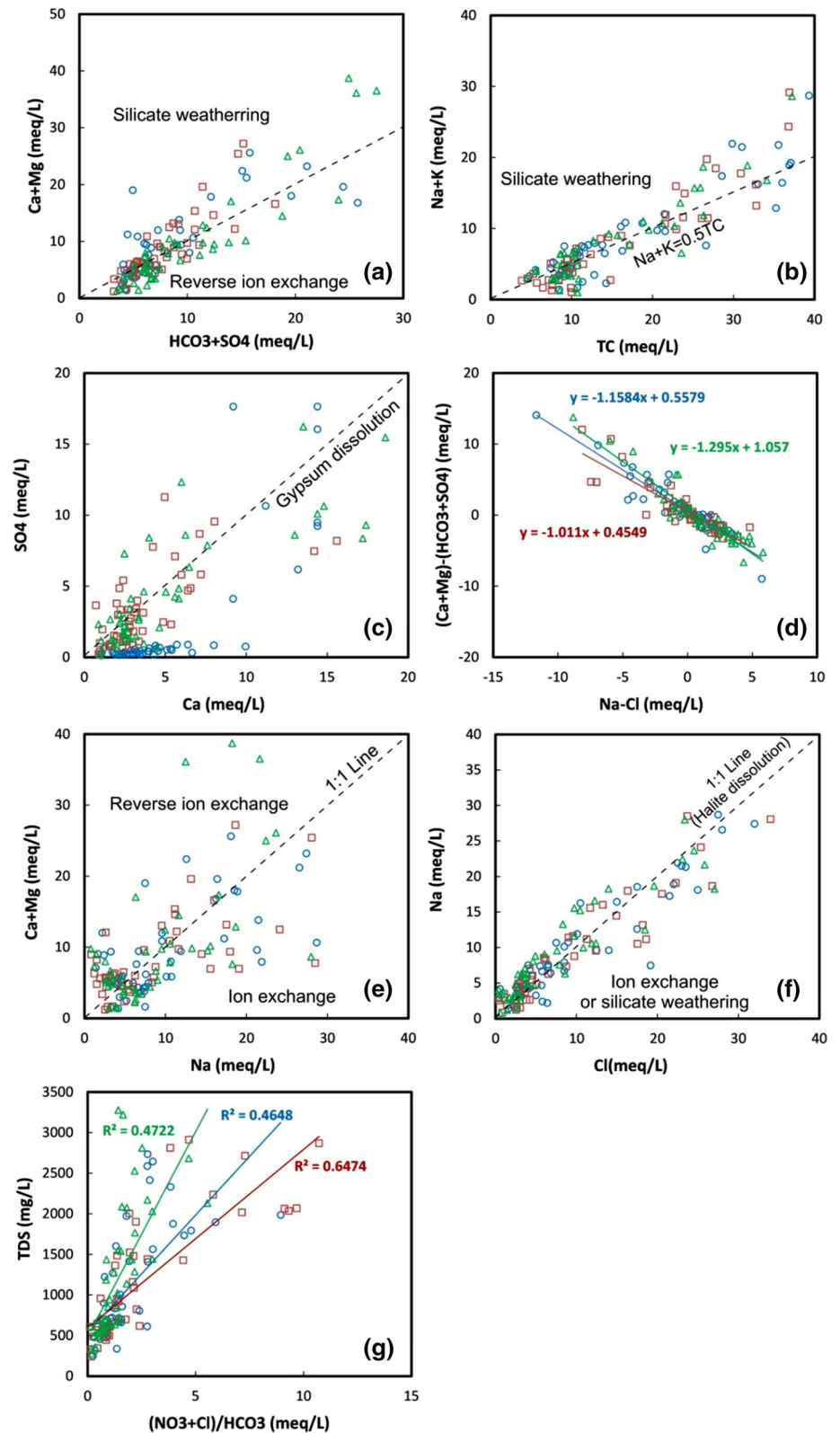
order to exploit potential correlations among parameters and to identify the dominant processes that control hydrogeochemistry. The exact number of factors was chosen by Kaiser criterion (1960) in which factors with eigenvalues smaller than 1 are eliminated; following this process, 6 factors were finally chosen that explain 81.7% of
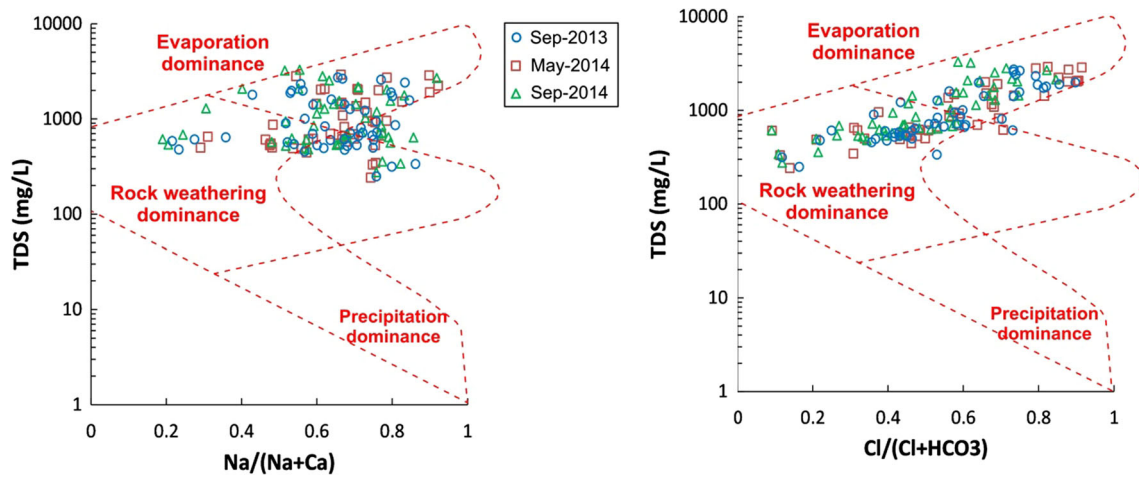
Fig. 8 Gibbs (1970) plots for groundwater samples of the three periods

Table 2 Sorted rotated factor loadings and communalities

Variable	Factor 1	Factor 2	Factor 3	Factor 4	Factor 5	Factor 6	Communality
Ca^{2+}	0.932	0.000	0.000	0.000	0.000	0.000	0.910
Mg^{2+}	0.908	0.000	0.000	0.000	0.000	0.000	0.860
Cl^-	0.907	0.000	0.000	0.000	0.000	0.000	0.897
Na^+	0.855	0.000	0.000	0.000	0.000	0.000	0.822
SO_4^{2-}	0.812	0.000	0.000	0.000	0.000	0.000	0.772
HCO_3^-	0.733	0.000	0.000	0.000	0.000	0.000	0.710
K^+	0.684	0.000	0.638	0.000	0.000	0.000	0.913
Pb	0.000	−0.917	0.000	0.000	0.000	0.000	0.882
Cd	0.000	−0.874	0.000	0.000	0.000	0.000	0.805
Mn	0.000	−0.665	0.000	0.000	0.000	0.000	0.509
Fe	0.000	−0.534	0.000	0.000	0.414	0.406	0.718
SiO_2	0.000	0.000	0.835	0.000	0.000	0.000	0.853
As	0.000	0.000	0.772	0.000	0.000	0.000	0.756
Cr	0.000	0.000	0.000	−0.829	0.000	0.000	0.909
NO_3^-	0.000	0.000	0.000	−0.757	0.000	0.000	0.824
Al	0.000	0.000	0.000	0.000	0.904	0.000	0.849
F^-	0.000	0.000	0.000	0.000	0.000	0.932	0.898
Variance	5.035	2.710	1.887	1.603	1.395	1.256	13.888
% variance	0.296	0.159	0.111	0.094	0.082	0.074	0.817

Insignificant loadings below 0.400 are shown as 0 for simplicity

total variance. Results of the FA are shown in Table 2, and the loading plot for the first two factors is shown in Fig. 9.

The first factor (FA1) explains 29.6% of total variance and includes with strong positive loadings the parameters of Ca^{2+}, Mg^{2+}, Cl^-, Na^+, SO_4^{2-}, HCO_3^- and with medium positive loading K^+; it is evident that this factor is related to the increased groundwater salinization which occurs due to irrigation water return flow. This process is typical in agricultural areas where the cumulative accumulation of ions in upper soil horizons increases salinity, especially when exploitation rate of groundwater used for

irrigation is significantly higher than the recharge of aquifer systems.

The second factor (FA2) expresses the impact from the felsic and intermediate igneous formations of the area (rhyolites, rhyolitic dacites and andesites); it explains 15.9% of total variance and includes with strong negative loadings the parameters of Pb and Cd and with medium negative loadings the parameters of Mn and Fe. The strong correlation among Pb and Cd (often accompanied by Zn) is frequent a good indication for a potential sulfide mineralization, a hypothesis which seems to be realistic for the
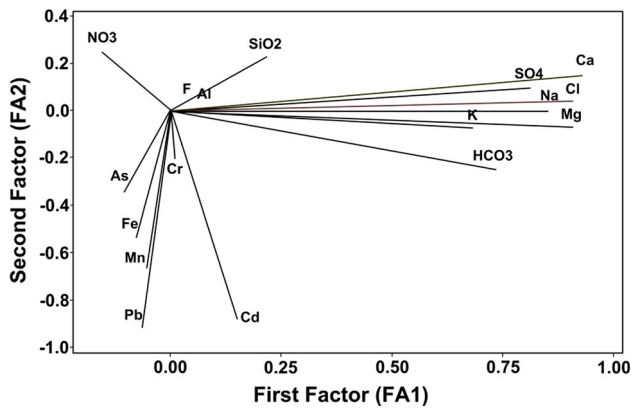
Fig. 9 Loading plot for the first two factors of the R-mode factor analysis

study area, based on the geological background of the substrate formations.

The third factor (FA3) explains 11.1% of total variance and includes with strong positive loadings Si and As and with medium positive loading K^+; this factor is also involved with the impact from the volcanic formations, but the occurrence of SiO_2 within its dominant parameters denotes that the nature of rocks involved is more felsic than those of FA2. However, no specific spatial pattern is identified for the samples affected by FA2 and FA3; thus, local geochemical composition of parent rocks and ongoing geochemical processes affecting the mobility of trace elements is believed to control hydrogeochemistry.

The fourth factor (FA4) explains 9.4% of total variance and includes Cr and NO_3^- with strong negative loadings; this factor possibly interprets the impact from irrational agricultural practices and unsustainable use of nitrogen fertilizers, which finally end up as nitrate ions in aquifer. Although there is no information about the speciation of Cr, it is believed that it exists in its hexavalent form which is far more mobile than the trivalent form in the geological environments; however, nitrates even though are considered as a potential oxidant for Cr(III) toward Cr(VI) formation, they are not efficient to provoke such redox processes in a basin scale; the co-occurrence of Cr and NO_3^- is more likely to be attributed to the specific characteristics of the porous aquifers systems which exist in the study area and are composed mainly by weathered materials, often from mafic parent rocks, which may host Cr-bearing altered minerals (e.g., serpentines). Those minerals are more susceptible to dissolution than other more stable forms (e.g., olivines) which are hosted in parent rocks; hence, the possibilities for Cr(VI) mobilization are higher in alluvial basin; in case of simultaneous agricultural activities, nitrate is also existing as an impact from the excessive use of fertilizers; hence, there is a correlation among Cr and NO_3^-, even though they are not directly related.

The fifth factor (FA5) explains 8.2% and includes Al and Fe with strong and weak positive loadings, respectively. It expresses the presence of Al–Fe oxides and hydroxides in the upper soil horizons, as a result of the weathering processes.

Finally, the sixth factor (FA6) explains 7.4% and includes with strong positive loading F^- and with medium one Fe. Since no geochemical analyses of parent rocks are available, fluorine origin is a matter of speculation; the two dominant sources in the study area could be either the felsic volcanic rocks in which F^- is present in mica minerals, or alternatively the clastic sedimentary formations (e.g., conglomerates with volcanic weathered material).

Hierarchical clustering analysis

The potential correlation among groundwater samples were explored with the use of a hierarchical cluster analysis (HCA). Samples were categorized into 2 clusters (C1 and C2) according to their squared Euclidean distance, and the results are shown in Fig. 10, while Table 3 contains their descriptive statistical parameters and Fig. 11 shows their spatial distribution.

The first cluster (C1) which contains the majority of samples (38 samples) is spatially located at the eastern and central parts of the plain, while C2 is situated mainly westward with few local exceptions. Based on their hydrogeochemical characteristics (Table 2), C2 factor expresses the groundwater samples which are impacted from salinization; hence, C1 mainly includes the majority of samples affected by FA1 of the previously mentioned factor analysis. The salinization effect can be justified by the elevated median values of EC (3151.6 μS/cm) and the elevated content of major ions like Ca^{2+}, Mg^{2+}, K^+, Na^+, SO_4^{2-} and Cl^- in respect of C1. In addition, pH values are slightly more alkaline (median = 7.5) compared to the neutral (median = 7) ones of C1. On the contrary, C1 clusters appear to have higher values of some trace metals like Pb and As, which are associated with the impact from the volcanic formations of the substrate as seen in FA2, FA3 and FA6 factors of FA analysis. However, it should be noted that NO_3^- concentrations (FA4), which is one of the dominant environmental pressures of the study area due to the intensive agriculture, appear to have nearly equal median values for the two clusters (14.7 and 11.6 mg/L, respectively); hence, nitrate contamination seems to be an individual contamination process which cannot be directly related or affected either with salinization or with volcanic formations weathering.

Fig. 10 Dendrogram of HCA for groundwater samples
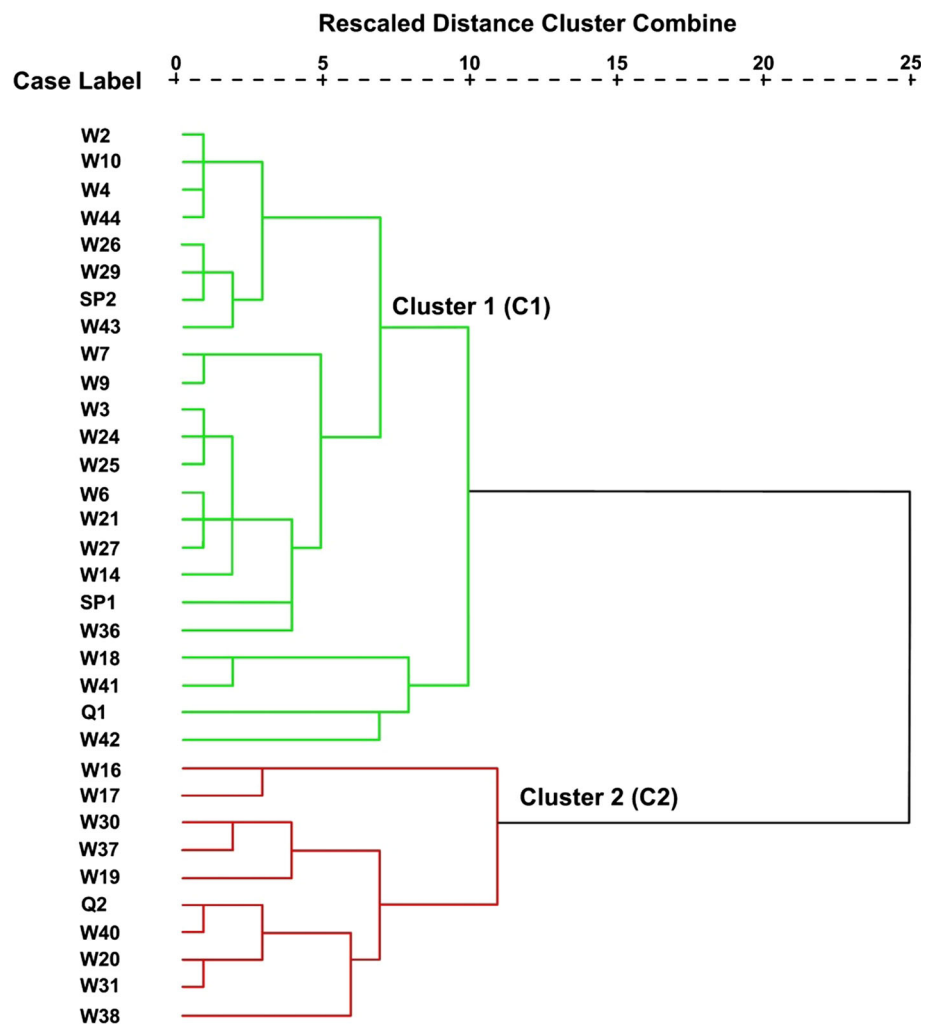
Conclusions

The results of the three sampling periods in the Marand plain show that the order of abundance of major cations is $Na^+ > Ca^{2+} > Mg^{2+} > K^+$ and of major anions is $HCO_3^{2-} > Cl^- > SO_4^{2-}$. Also, in respect of the trace metals, their median values follow the decreasing concentration order: $Al > Fe > As > Pb > Cr > Mn > Cd$. The values of EC range between 377 and 5120 µS/cm for all three sampling periods; the elevated EC values >2500 µS/cm are indicative for the existence of increased groundwater salinization.

Piper diagrams show that the majority of samples belong to Na–Cl water type and are followed by Ca–HCO$_3$ and mixed Ca–Na–HCO$_3$. Spatially the most saline groundwaters expressed by the Na–Cl water type are located mainly in the northern and eastern parts of the plain. Mixed water types are located in inner plain areas, denoting a succession with the saline waters due to ion exchange and reverse ion exchange processes. Recharge areas, expressed by Ca–HCO$_3$ type, seem to follow a SE–NW direction across the eastern and central plain areas, implying a potential groundwater flow path.

Cross-plots show that weathering and dissolution of different rocks and minerals, e.g., carbonates, silicates, gypsum and halite, ion exchange, reverse ion exchange and anthropogenic activities, especially agricultural activities, influence the hydrogeochemistry of the study area.

As a result, the FA reveals that 6 factors with 81.7% of total variance impacts in the overall hydrogeochemistry. The FA1 demonstrates the increased groundwater salinization which occurs due to irrigation water return flow. The FA2 and FA3 express the impact from the felsic and intermediate igneous formations of the area. The FA4 interprets the impact from irrational agricultural practices and unsustainable use of nitrogen fertilizers, which finally end up as nitrate ions in aquifer. The FA5 expresses the presence of Al–Fe oxides and hydroxides in the upper soil horizons, as a result of the weathering processes. The FA6 explains the origin of

Table 3 Descriptive statistical parameters of the samples of cluster 1 and 2

Variable	Unit	Cluster 1				Cluster 2			
		Min.	Median	Max.	SD	Min.	Median	Max.	SD
pH	–	6.8	7.5	7.9	0.2	5.9	7.0	7.4	0.5
EC	µS/cm	398.0	986.0	2950.0	586.3	2310.0	3151.6	4546.6	806.9
Ca^{2+}	mg/L	19.2	59.3	97.2	19.2	108.5	175.7	315.3	60.7
Mg^{2+}	mg/L	4.9	34.2	74.5	18.3	40.1	94.3	179.5	36.7
Na^{+}	mg/L	29.3	108.4	427.2	100.8	219.1	372.6	569.5	104.6
K^{+}	mg/L	1.7	4.6	13.4	2.7	4.6	6.5	21.9	6.5
HCO_3^{-}	mg/L	200.1	253.6	468.8	79.6	152.9	408.8	613.5	145.6
SO_4^{2-}	mg/L	8.2	69.5	147.6	31.7	115.0	377.6	696.8	161.8
Cl^{-}	mg/L	16.1	124.8	611.6	149.3	345.7	557.1	931.9	203.7
NO_3^{-}	mg/L	6.6	14.7	39.1	9.2	3.7	11.6	27.6	7.6
SiO_2	mg/L	3.4	21.3	44.7	10.5	6.6	15.4	51.7	17.0
F^{-}	mg/L	0.2	0.4	1.8	0.4	0.4	0.5	1.6	0.3
Cr	µg/L	0.0	2.7	18.0	3.6	0.0	3.4	6.1	1.8
Pb	µg/L	1.7	10.0	20.8	4.8	2.3	6.1	17.3	4.9
Cd	µg/L	0.1	1.6	5.1	1.3	0.6	1.2	5.6	1.6
Mn	µg/L	0.3	2.6	607.0	153.2	0.5	5.8	176.0	50.7
Al	µg/L	0.0	34.7	372.0	83.4	0.0	48.5	581.3	164.9
Fe	µg/L	7.3	45.6	339.5	81.6	12.2	46.6	219.6	56.8
As	µg/L	0.3	11.7	19.3	5.6	0.6	6.7	16.7	5.6

Fig. 11 Spatial distribution of the groundwater samples of associated clusters (C1–C2)
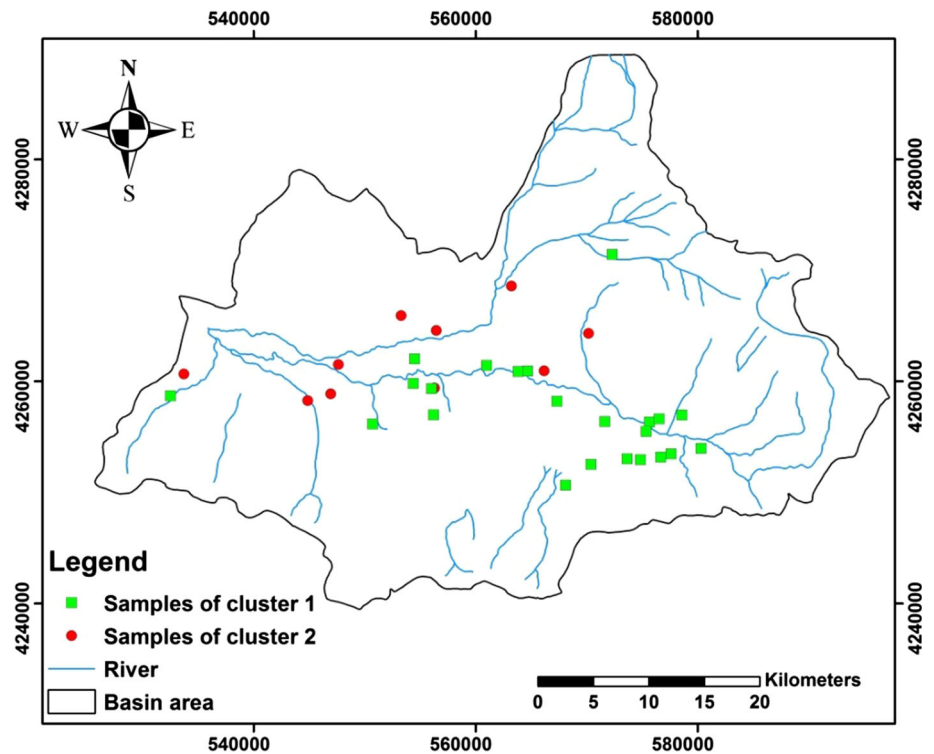
F^{-}, which is present in mica minerals, or alternatively the clastic sedimentary formations.

The results of HCA distinguish two distinct clusters of groundwater samples. Samples of cluster C1, which appear to have higher values of some trace metals like Pb and As, are spatially located at the eastern and central parts of the plain. These high values can be associated with the impact from the volcanic formations of the substrate. Samples of

cluster C2, which express the salinization of the groundwater, are situated mainly westward with few local exceptions.

References

Al-Qudah O, Woocay A, Walton J (2011) Identification of probable groundwater paths in the Amargosa Desert vicinity. Appl Geochem 26:565–570

APHA (2005) Standard methods for the examination of water and wastewater, 21st edn. American Public Health Association, Washington DC

Appelo CAJ, Postma D (1993) Geochemistry, groundwater and pollution. A.A Balkema, Brookfield

Arumugam K, Elangovan K (2009) Hydrochemical characteristics and groundwater quality assessment in Tirupur region, Coimbatore district, Tamil Nadu, India. Environ Geol 58:1509–1520

Barzegar R, Asghari Moghaddam A, Najib M, Kazemian N, Adamowski J (2016) Characterization of hydrogeologic properties of the Tabriz plain multi-layer aquifer system, NW Iran. Arab J Geosci 9(2):1–17

Berberian M (1976) Contribution to the seismotectonics of Iran (part II). Geological Survey of Iran, Rep. No. 39, 518 P.5 Maps. 259 Figures

Bhuiyan M, Rakib MA, Dampare SB, Ganyaglo S, Suzuki S (2011) Surface water quality assessment in the central part of Bangladesh using multivariate analysis. KSCE J Civil Eng 15(6):995–1003

Birke M, Rauch U (1993) Environmental aspects of the regional geochemical survey in the southern part of East Germany. J Geochem Explor 49(1–2):35–61

Dalton MG, Upchurch SB (1978) Interpretation of hydrochemical facies by factor analysis. Ground Water 16(4):228–233

Datta PS, Tyagi SK (1996) Major ion chemistry of groundwater in Delhi area: chemical weathering processes and groundwater flow regime. J Geol Soci India 47:179–188

Devic G, Djordjevic D, Sakan S (2014) Natural and anthropogenic factors affecting the groundwater quality in Serbia. Sci Total Environ 468–469:933–942

Domenico PA, Schwartz FW (1998) Physical and chemical hydrogeology, 2nd edn. John Wiley and Sons Inc, New York, p 506

Eftekhar Nezhad AJ, Ghorashi M, Mehrparto M, Arshadi S, Zohrehbakhsh A (1991) Geology map of Tabriz 1:250000 sheets. Geological Survey of Iran

Elango L, Kannan R (2007) Rock–water interaction and its control on chemical composition of groundwater: chapter 11. Dev Environ Sci 5:229–243

Fakhri MS, Asghari Moghaddam A, Najib M, Barzegar R (2015) Investigation on n concentrations in groundwater resources of Marand plain and groundwater vulnerability assessment using AVI and GODS methods. J Environ Stud 41(73):14–16

Fisher RS, Mulican WF (1997) Hydrogeochemical evolution of sodium sulphate and sodium-chloride groundwater beneath the Northern Chihuahua desert, Trans-Pecos, Texas, USA. Hydrogeol J 10(4):455–474

Fitzpatrick ML, Long DT, Pijanowski BC (2007) Exploring the effects of urban and agricultural land use on surface water chemistry, across a regional watershed, using multivariate statistics. Appl Geochem 22:1825–1840

Gibbs RJ (1970) Mechanisms controlling world water chemistry. Science 17:1088–1090

Han G, Liu C-Q (2004) Water geochemistry controlled by carbonate dissolution: a study of the river waters draining karst-dominated terrain, Guizhou province, China. Chem Geol 204:1–21

Hardle W, Simar L (2007) Applied multivariate statistical analysis, 2nd edn. Springer, Berlin

Hassen I, Hamzaoui-Azaza F, Bouhlila R (2016) Application of multivariate statistical analysis and hydrochemical and isotopic investigations for evaluation of groundwater quality and its suitability for drinking and agriculture purposes: case of Oum Ali-Thelepte aquifer, central Tunisia. Environ Monit Assess 188:135

Helena B, Pardo R, Vega M, Barrado E, Fernandez JM, Fernandez L (2000) Temporal evolution of groundwater composition in an alluvial aquifer (Pisuerga River, Spain) by principal component analysis. Wat Res 34:807–816

Hernandez MA, Gonzalez N, Levin M (1991) Multivariate analysis of a coastal phreatic aquifer using hydrochemical and isotopic indicators, Buenos Aires, Argentina. In: Proceedings of the international association on water pollution research and control's international seminar on pollution, protection and control of groundwater, as published in water science and technology. vol 24, pp 139–146

Jalali M (2006) Chemical characteristics of groundwater in parts of mountainous region, Alvand, Hamadan, Iran. Environ Geol 51:433–446

Jalali M (2009) Geochemistry characterization of groundwater in an agricultural area of Razan, Hamadan, Iran. Environ Geol 56:1479–1488

Khaleghi F, Shahverdizadeh GH (2014) Hydrogeochemical characteristics and evaluation of the drinking and irrigation water quality in Marand Plain, East Azerbaijan, NW Iran. Br J Appl Sci Technol 4(17):2458–2467

Kumar M, Rmanathan AL, Rao MS, Kumar B (2006) Identification and evaluation of hydrogeochemical processes in the groundwater environment of Delhi, India. Environ Geol 50:1025–1039

Lawrence FW, Upchurch SB (1982) Identification of recharge areas using geochemical factor analysis. Ground Water 20:680–687

Li P, Jianhua W, Hui Q (2013) Assessment of groundwater quality for irrigation purposes and identification of hydrogeochemical evolution mechanisms in Pengyang County, China. Environ Earth Sci 69:2211–2225

Lokhande PB, Patit VV, Mujawar HA (2008) Multivariate statistical analysis of ground water in the vicinity of Mahad industrial area of Konkan region, India. Int J Appl Environ Sci 3(2):149–163

Manouchehri GH (2000) Water crisis in Iran. Iran Water Environ J. No. 39

McKenna JE (2003) An enhanced cluster analysis program with bootstrap significance testing for ecological community analysis. Environ Model Softw 18(2):205–220

Motiee H, Monouchehri GH, Tabatabai MRM (2001) Water crisis in Iran, codification and strategies in urban water. In: Proceedings of the workshops held at the UNESCO symposium, technical documents in hydrology, vol 45, pp 55–62

Nabavi MH (1976) An introduction to the geology of Iran. Tehran: geological survey of Iran, p 109 (**in Persian**)

Nesrine N, Rachida B, Ahmed A (2015) Multivariate statistical analysis of saline water—a case study: Sabkha Oum LeKhialate (Tunisia). Int J Environ Sci Develop 6(1):40–43

Otto M (1998) Multivariate methods. In: Kellner R, Mermet JM, Otto M, Widmer HM (eds) Analytical chemistry. Wiley-VCH, Weinheim

Pandey RK (2016) Quantitative studies on physico- chemical properties of ground water of Agra (Uttar Pradesh) India. World J Biol Med Sci 3(1):132–136

Pazand K, Hezarkhani A, Ghanbari Y, Aghavali N (2012) Geochemical and quality assessment of groundwater of Marand Basin, East Azarbaijan Province, northwestern Iran. Environ Earth Sci 67:1131–1143

Pereira HG, Renca S, Sataiva J (2003) A case study on geochemical anomaly identification through principal component analysis supplementary projection. Appl Geochem 18:37–44

Pichaiah S, Senthil Kumar GR, Srinivasamoorthy K, Sarma VS (2015) Hydrochemical characterization and quality assessment of Groundwater in Tirupur Taluk, Tamil Nadu, India: emphasis on irrigation utility. J Acad Ind Res 1(12):805–812

Rajmohan N, Elango L (2004) Identification and evolution of hydrogeochemical processes in an area of the Palar and Cheyyar River Basin, Southern India. Environ Geol 46:47–61

Sadashivaiah C, Ramakrishnaiah CR, Ranganna G (2008) Hydrochemical analysis and evaluation of groundwater quality in Tumkur Taluk, Karnataka State, India. Int J Environ Res Pub Health 5(3):158–164

Sajil Kumar PJ (2014) Evolution of groundwater chemistry in and around Vaniyambadi Industrial Area: differentiating the natural and anthropogenic sources of contamination. Chem Erde 74(4):641–651

Senthilkumar M, Elango L (2013) Geochemical processes controlling the groundwater quality in lower Palar river basin, southern India. J Earth Syst Sci 122(2):419–432

Stallard RF, Edmond JM (1983) Geochemistry of the Amazon 2: the influence of the geology and weathering environment on the dissolved load. J Geophys Res 88:9671–9688

Subramani T, Rajmohan N, Elango L (2010) Groundwater geochemistry and identification of hydrogeochemical processes in a hard rock region, southern India. Environ Monit Assess 162:123–137

Tarki M, Dassi L, Hamed Y, Jedoui Y (2011) Geochemical and isotopic composition of groundwater in the Complex Terminal aquifer in southwestern Tunisia, with emphasis on the mixing by vertical leakage. Environ Earth Sci 64:85–95

Tiwari AK, Singh AK (2014) Hydrogeochemical investigation and groundwater quality assessment of Pratapgarh District, Uttar Pradesh. J Geol Soc India 83:329–343

Tziritis E (2014) Environmental monitoring of Micro Prespa Lake basin (Western Macedonia, Greece). Hydrogeochemical characteristics of water resources and quality trends. Environ Monit Assess 186(7):4553–4568

Varol S, Davraz A (2015) Evaluation of the groundwater quality with WQI (water quality index) and multivariate analysis: a case study of the Tefenni plain (Burdur/Turkey). Environ Earth Sci 73(4):1725–1744

Venugopal T, Giridharan L, Jayaprakash M, Periakali P (2009) Environmental impact assessment and seasonal variation study of the groundwater in the vicinity of river Adyar, Chennai, India. Environ Monit Assess 149:81–97

Ward JH (1963) Hierarchical grouping to optimize an objective function. J Am Stat Assoc 301:236–244

Yidana SM, Ophori D, Banoeng-Yakubo B (2008) A multivariate statistical analysis of surface water chemistry—the Ankobra Basin, Ghana. J Environ Manag 86:80–87

Yidana SM, Banoeng-Yakubo B, Sakyip PA (2012) Identifying key processes in the hydrochemistry of a basin through the combined use of factor and regression models. J Earth Sys Sci 121(2):491–507